N91-10480

FIRE CIRRUS ON 10/28/86: LANDSAT; ER-2; KING AIR; THEORY

Bruce A. Wielicki and John T. Suttles
Atmospheric Sciences Division
NASA Langley Research Center
Hampton, VA. 23665-5225

Andrew J. Heymsfield
National Center for Atmospheric Research
Boulder, CO. 80302

Ronald M. Welch
South Dakota School of Mines and Technology
Rapid City, SD. 57701

James D. Spinhirne
NASA Goddard Space Flight Center
Greenbelt, MD. 20771

Lindsay Parker and Robert F. Arduini
Planning Research Corporation
Hampton, VA. 23602

I. INTRODUCTION

The purpose of this study is to conduct a simultaneous examination of cirrus clouds in the FIRE Cirrus IFO-I on 10/28/86 using a multitude of remote sensing and in-situ measurements. The focus of the study is cirrus cloud radiative properties and their relationship to cloud microphysics. A key element of this study is the comparison of radiative transfer model calculations and varying measured cirrus radiative properties (emissivity, reflectance vs. wavelength, reflectance vs. viewing angle). As the number of simultaneously measured cloud radiative properties and physical properties increases, more sharply focused tests of theoretical models are possible.

II. CALIBRATION AND NAVIGATION

The area of interest is shown in Figure 1 using the Landsat 11.5μm brightness temperature. The region shown is 2048 by 2048 pixels with a length of 58.4 km on a side. Time of the Landsat overpass is 1553 GMT on 10/28/86. Calibration for all Landsat channel radiances is taken from Markham and Barker (1986). Absolute accuracy of solar reflectance bands is estimated as 10 percent of any radiance value.

Figure 1 also gives the aircraft tracks of the ER-2 and King Air aircraft. Nominal navigation accuracy for Landsat and aircraft is 1 km. The King Air track (curved in Figure 1) has been advected using the King Air wind measurements (7.3 km altitude), in order to compensate for the cloud motion between the time of the aircraft observations and the time of the Landsat overpass. Typical wind speeds are 16 m sec^{-1} from the west (270°), giving a largest advection distance of 15 km for the King Air data at 1536 GMT shown at the top of Figure 2. The opposite end of the King Air track required a correction of 1 km.

The ER-2 observations are taken within ± 2 minutes of 1553 GMT and require maximum wind corrections of 2 km. For all multiple platform intercomparisons, radiance data from the ER-2 and Landsat are spatially averaged to 1 km resolution in order to reduce the effect of noise from limitations in navigation accuracy and time simultaneity.

III. NADIR REFLECTANCE VERSUS 11.5μm EMISSIVITY

Figure 2 gives the observed nadir reflectance R versus 11.5μm effective emissivity ϵ using the Landsat radiances along the ER-2 groundtrack (data given as points). Nadir reflectance is calculated as an equivalent Lambertian reflectance, $R = \pi L/S_0 \cos\theta_0$, where L is spectral radiance ($Wm^{-2}sr^{-1}\mu m^{-1}$), S_0 is solar spectral flux ($Wm^{-2}\mu m^{-1}$) averaged over the narrow spectral bandpass, and θ_0 is the solar zenith angle (63°). Effective emissivity is calculated following Platt et al (1980), $\epsilon = (L_{clr} - L_m)/(L_{clr} - L_{cld})$ where L_m is the measured 11.5μm radiance, L_{clr} is the clear-sky 11.5μm radiance determined using the apparently clear area in the lower right of Figure 2, and L_{cld} is the blackbody radiance which would be emitted by an optically thick cloud at the altitude of the cirrus layer. Cloud altitude is determined using the ER-2 lidar data.

Backscatter crossections from the ER-2 downlooking lidar give two cloud layers beneath the ER-2. The lower cloud layer is between 6.9 and 8.0 km altitude, while the upper layer is between 8.9 and 11.2 km altitude. An examination of optically thick portions of the cloud field (nadir 0.83μm reflectance between 50% and 60%) using the Landsat 10.8μm channel data gave an emitting temperature of 231K, which the Green Bay radiosonde places at an altitude of 9.0 km. This would place an optically thick cirrus cloud layer at an altitude where no cirrus was visible in the lidar backscatter, a puzzling result. One possibility for the discrepancy in these results is that the optically thick brightness temperature measured by the Landsat (and ER-2) radiometers was produced by a combination of an optically thick lower layer with cloud top at 8 km and an optically thin overlying cirrus at 9-11 km. In this initial work, an 9.0 km cloud height is used for emissivity calculations. If the appropriate cloud altitude were in fact 7.5 km, or 10.0 km, an error of ± 15% in 11μm emissivity would occur.

Figure 2 compares the measured 0.83μm reflectance vs 11μm emissivity to theoretical calculations. In order to make the model and measurements more directly comparable, the first order reflectance of the surface (Lake Michigan) has been removed as described in Platt et al (1980). This correction causes the data to tend to zero reflectance and zero emissivity as cloud optical depth tends to zero. The correction is approximately 4% in nadir reflectance for small optical depths, decreasing to no correction for large optical depths. The theoretical results are shown for calculations of cloud albedo using a Delta-Eddington approximation with single scattering albedo = 1.0; asymmetry factor g = 0.88 for spherical drops and g = 0.73 for cylindrical ice particles; and the ratio of scattering optical depth at 0.83μm $\tau_s(0.83)$ to absorption optical depth at 11.4μm $\tau_a(11.4)$ is taken as $\tau_a(11.4)/\tau_s(0.83) = 0.57$ for spheres and 0.50 for cylinders. These parameters are those used in Platt et al (1980). In all modeled results, emissivity is absorption emissivity. Wielicki (1980) showed that effective nadir emissivity is within 1% of absorption emissivity for 11.5μm radiation in spherical ice clouds 20μm mode radius, using ATRAD adding doubling calculations (Wiscombe, 1975). Finally, multiple scattering calculations were performed using the Finite Difference method (Barkstrom, 1976) as extended by Suttles (1986). The Finite Difference method produced estimates of nadir relfectance meant to be directly comparable to the Landsat reflectance. The Finite Difference code was run using a single scattering albedo of 1.0 and a double Heyney-Greenstein phase function with parameters b=0.98, g_1=0.9, and

g_2= -0.5. Figure 3 compares this phase function with a single H-G phase function (g=0.9) and with two phase functions from Liou, 1973 for Mie calculations of spherical water drops, and for theoretical calculations for randomly oriented cylinders. In general, the cylinders exhibit much more side scattering (60 to 120° scattering angles) than do spheres. The double H-G phase function is intermediate between the sphere and cylinder phase functions. Note that for single scatter, radiation scattered from the solar zenith angle of 63° to nadir for Landsat would have a scattering angle of 117°, where large differences in the three phase functions occur. Figure 2 indicates that the measured nadir reflectances are much larger than those predicted using the double H-G, indicating larger side scattering, more consistent with the cylindrical phase function. Figure 2 also demonstrates the large anisotropy of reflected radiation for thin cirrus. Albedo is much larger than nadir reflectance (Finite Difference albedo is very similar to the Delta-Eddington values for spheres), indicating the importance of using multiple-scattering calculations capable of determination of viewing zenith and azimuth variations of reflected radiation (see also King, 1987). Future work will investigate Mie calculations using the observed King Air microphysical measurements, and hexagonal ice crystal phase functions.

IV. MULTIPLE ANGLE VIEWS OF CIRRUS

Given the large differences between nadir reflectance and albedo for optically thin cloud, an additional independent test of theoretical calculations is their ability to predict the reflectance anisotropy as a function of viewing zenith angle and viewing azimuth angle. A particularily useful test is the determination of the ratio of reflectance at two viewing angles of the same cloud. This ratio eliminates sensitivity to uncertainties in the absolute gain calibration of the radiometer. The ER-2 flight path on 10/28/86 was chosen to provide observations as a function of angle in the solar plane (i.e. viewing azimuth angle of 0° (forward scatter) while scanning to the right of the aircraft, and 180° (backward scatter) while scanning to the left of the aircraft). Figure 4 gives a schematic of the geometry for the Landsat/ER-2 intercomparison.

The first step in this process is to use the nadir ER-2 observations to intercalibrate the ER-2 and Landsat radiometers. After navigation, a regression of 1-km averaged ER-2 and Landsat radiances gave R(ER-2) = 0.779*R(Landsat) - 1.61 (units of nadir reflectance) with a 2σ uncertainty in the gain of $\pm$ .025 and correlation coefficient of 0.993. While the final agreement between the radiometers is good, the relative gain differences in these two radiometers at 0.83μm is larger than expected. More careful calibrations of narrowband radiometers are recommended for future work.

Having navigated and intercalibrated the Landsat and ER-2 radiometer data at nadir, off nadir observations at 30° were examined. In view of the presence of two cloud layers, and lack of lidar data for off nadir viewing, the 30° viewing zenith data was navigated using test cloud altitudes between 6.5 and 12.5 km. Spatial variations in the 30° viewing zenith ER-2 data matched those in the nadir Landsat view when cloud height was set to 7.5 km, in the center of the lower cloud layer. Poor correlations were found assuming cloud heights within the upper cloud layer. This test indicates that the shortwave radiative properties are dominated by the lower cloud level, consistent with microphysical measurements showing increasing ice water content with decreasing cloud height.

After subtracting off the surface reflectance contribution as in section III, measured cloud reflectance ratios $R(\theta=30,\phi=0)/R(\text{nadir})$ ranged from 1.3 to 1.5, where θ is viewing zenith angle and ϕ is viewing azimuth angle relative to the solar plane (ϕ=0 is forward scatter). Cloud reflectance ratios for

backscattered radiation R(θ=30,ϕ=180)/R(nadir) ranged from 0.8 to 1.2. Theoretical calculations for the reflectance ratios using the Finite Difference model discussed in section III are shown in Figure 5, and show more anisotropy in both forward and backscatter ratios than the data. Recall that the scattering optical depth given in Figure 5 is approximately twice the absorption optical depth at 11.4μm, so that scattering optical depth 1 is approximately an emissivity at 11.4μm of 1-exp(-0.5) = 0.39, typical of the data shown in Figure 2. Note that the reflectance ratio is a strong function of optical depth in Figure 5, indicating the importance of cloud optical depth when using radiance (i.e. bidirectional reflectance) to estimate flux. This might impact the accuracy of ERBE derived fluxes for optically thin cirrus cloud.

V. NADIR REFLECTANCE: VISIBLE AND NEAR-INFRARED WAVELENGTHS

Theoretical calculations predict that cloud reflectance in near-infrared windows such as those at 1.6μm and 2.2μm should give lower reflectances than at visible wavelengths. The reason for this difference is that ice and liquid water show significant absorption at these wavelengths, in contrast to the nearly conservative scattering at visible wavelengths. In addition, because the amount of absorption scales with the thickness of the particle, increasing cloud particle size should lead to decreasing reflectances at 1.6μm and 2.2μm. Measurements of these wavelengths have to date, however, given unpredicted results (Twomey, 1982; Curren et al, 1982).

The Landsat satellite has channels with central wavelengths at 0.83μm, 1.65μm, and 2.21μm which cover this range of variation in cloud absorption. Figure 6 gives the ratio R(2.21μm)/R(0.83μm) for the Nadir Landsat data along the King Air ground track. At 153830GMT (at 13.7 km on the distance scale in Figure 6, the King Air aircraft took a direct sample of the cloud particles and found almost entirely water droplets, approximately 5-10μm in radius. This corresponds to the large anisotropic ratio (near 0.75) found in the Landsat data. A second direct cloud particle sample was collected at 1552GMT, consisting strictly of ice particles (broken spatial plates and some columns, 20 to 300μm in length). This second sample corresponds to a distance of 88 km in Figure 6 and shows a low measured reflectance ratio ($\approx$0.5).

Figure 7 compares theoretical calculations using the Finite Difference radiative transfer model with the measured nadir reflectance at 0.82 and 2.2μm along the King Air groundtrack. It is evident that there are two distinct populations of cloud particles along the 88 km track. The high reflectance ratio values in Figure 6 appear along the diagonal of nearly equal reflectance at the two wavelengths and are consistent with water or ice droplets with mode radius of 7.5μm or less. The remaining data indicates larger particles of about 30μm mode radius. Examination of the 1.6μm versus 2.2μm data indicate that the 7.5μm particles are water as opposed to ice. Further work using the King Air microphysical data along this groundtrack will allow determination of the effective particle size of the ice crystals in the lower cloud. The Sabreliner will provide microphysical data for the upper cirrus level, although on a different flight path.

VI. CONCLUSIONS

The 10/28/86 data provides a unique opportunity to compare measured and theoretical cloud properties for cirrus clouds. Overall impressions from the present analysis are:

1. The cirrus clouds produced more side-scattered radiation (scattering angle 60°-120°) than predicted by spherical particles. Cylindrical particle scattering appears to better describe the cirrus properties.

2. Variation of measured cloud reflectance at 0.82μm versus 2.21μm was consistent with King Air cloud particle samples, and in reasonable agreement with theoretical calculations.
3. The lower cirrus layer (7-8 km) appeared to dominate the cloud radiative properties as viewed by the ER-2 and Landsat. Initial indications from King Air and Sabreliner microphysics confirm the larger ice water contents in the lower cloud layer.
4. Better calibrations of narrowband shortwave radiometry are desired.

Future work will test use measured cirrus microphysical properties to determine phase functions used in the radiative transfer calculations, and to compare measured particle size to ratios of visible and near-infrared reflected solar radiation.

VII. REFERENCES

Barkham, B. L. and J. L. Barker, 1986, Landsat Technical Notes, August 1986.
Barkstrom, B. R., 1976: JQSRT, 16, 725-739.
Curren, R. J. and M. L. C. Wu, 1982: JAS, 39, 635-647.
King, M. D., 1987: JAS, 44, 1734-1751.
Liou, K. N., 1973: JGR, 78, 1409-1418.
Platt, C. M. R., et al., 1980: MWR, 108, 195-204.
Suttles, J. T., 1985: In Radiative Transfer in Scattering and Absorbing Atmospheres. Edited by J. Lenoble, A. Deepak Publishing.
Twomey , S. and T. Cocks, 1982: JMSJ, 60, 583-592.
Wiscombe, W., 1975: Climate of the Arctic, G. Weller and S. Bowling, Eds., University of Alaska Press, 245-254.

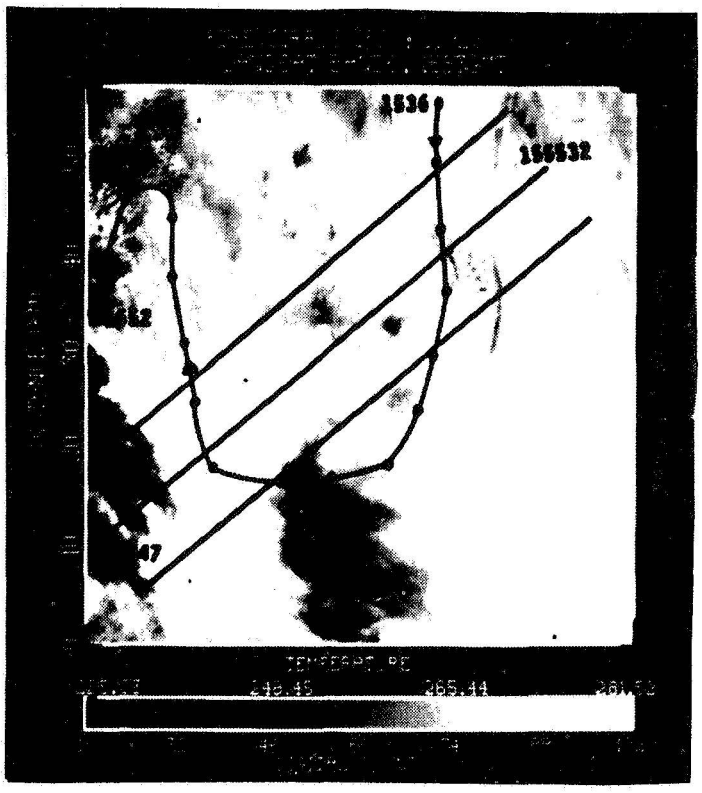

Figure 1

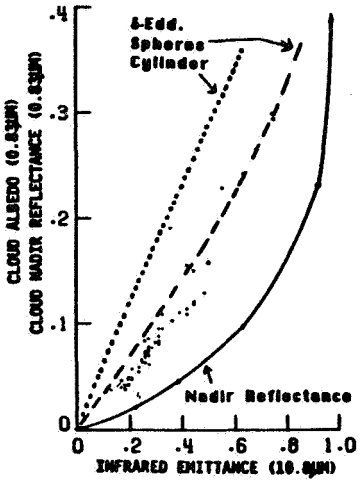

Figure 2

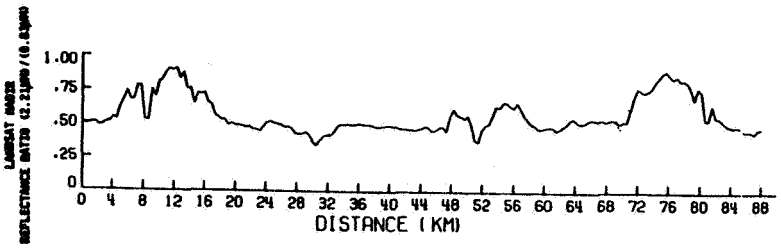

Figure 6

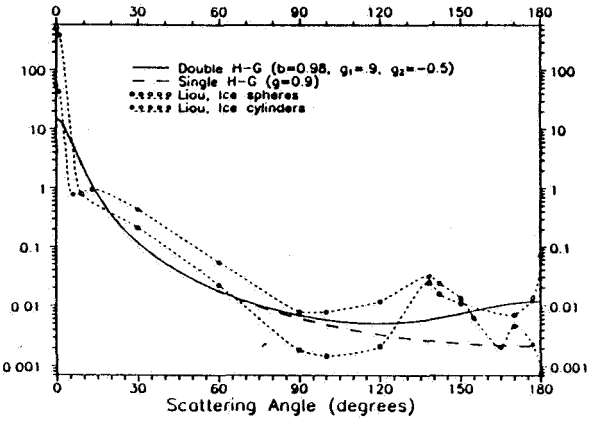

Figure 3

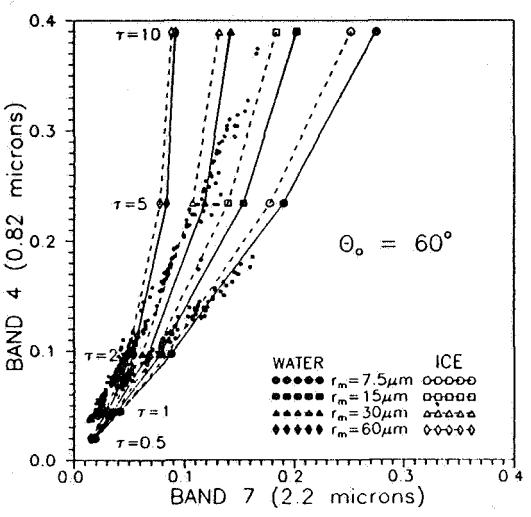

Figure 7

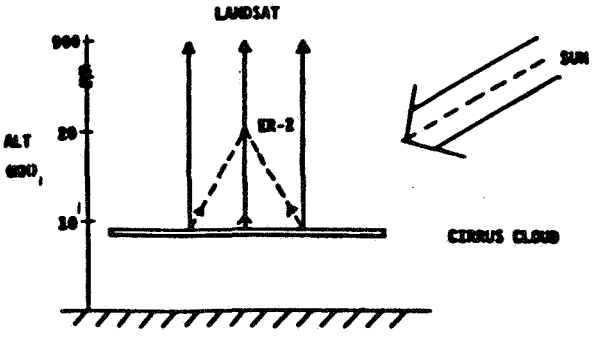

Figure 4

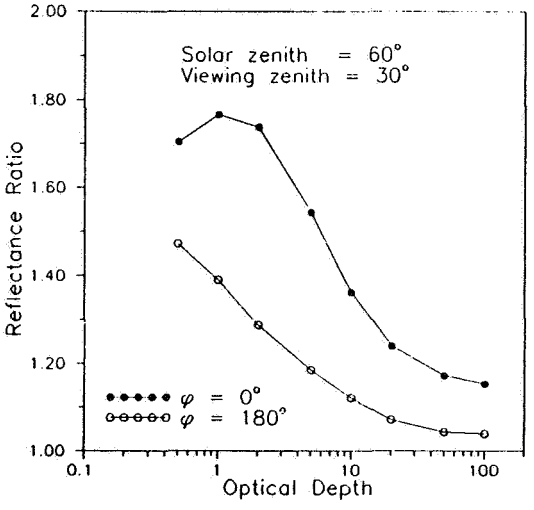

Figure 5